Korean J. Chem. Eng., 36(3), 439-449 (2019)
DOI: 10.1007/s11814-018-0214-6

pISSN: 0256-1115
eISSN: 1975-7220

Synthesis and performance evaluation of zeolitic imidazolate framework-8 membranes deposited onto alumina hollow fiber for desalination

Nizar Mu'ammar Mahpoz*, Norfazliana Abdullah*, Mohamad Zahir Mohd Pauzi*, Mukhlis A. Rahman*,†, Khairul Hamimah Abas, Azian Abd Aziz***, Mohd Hafiz Dzarfan Othman*, Juhana Jaafar*, and Ahmad Fauzi Ismail***

*Advanced Membrane Technology Research Centre (AMTEC), Universiti Teknologi Malaysia 81310 Skudai, Johor, Malaysia
**Department of Control & Instrumentation Engineering, Faculty of Electrical Engineering, Universiti Teknologi Malaysia, 81310 Skudai, Johor, Malaysia
***Language Academy, Universiti Teknologi Malaysia, 81310 Skudai, Johor, Malaysia
(*Received 8 July 2018 • accepted 18 December 2018*)

Abstract—This work describes the development of zeolitic imidazolate framework-8 (ZIF-8) membranes on modified alumina hollow fiber for desalination by forward osmosis. Effects of different seeds (ZnO, NiO and PDA) and sodium formate on in-situ deposition of ZIF-8 were studied in relation to the membrane's morphology and performance. XRD result shows that ZIF-8 was successfully synthesized in the presence of sodium formate. FESEM images showed PDA modified support was unsuccessful in producing well defined and dense ZIF-8 membrane layer even after another ZIF-8 re-deposition due to its minimal amount. The NiO modified support was also found unsuccessful, as ZIF-8 crystals were formed in clusters. On the contrary, dense ZIF-8 membrane was successfully prepared on ZnO modified support with SF-1 synthesis solution producing bigger ZIF-8 crystal and thinner ZIF-8 membrane than as of SF-2. Water flux performance in forward osmosis showed that NiO/ZIF-8, PDA/ZIF-8 and PDA/ZIF-8 (re-deposition) membranes gave negative water fluxes of $-50\ kg/m^2{\cdot}h$, $-5.2\ kg/m^2{\cdot}h$ and $-1.7\ kg/m^2{\cdot}h$ with reverse solutes of 42.66 $mol/m^2{\cdot}h$, 27.42 $mol/m^2{\cdot}h$ and 3.22 $mol/m^2{\cdot}h$, respectively, indicating the solute from draw solution diffused into the feed solution. However, ZIF-8 membrane prepared using SF with molar ratio of 1, on the ZnO modified support had a water flux of 13.3 $kg/m^2{\cdot}h$, reverse solute of 0.95 $kg/m^2{\cdot}h$ and salt rejection of 52.1%. When the SF ratio was increased to 2, the ZIF-8 membranes showed a water flux of 12.5 $kg/m^2{\cdot}h$, reverse solute of 1.64 $kg/m^2{\cdot}h$ and salt rejection of 54.9%. The moderate salt rejection could be associated with defects in the ZIF-8 membranes due to poor grain boundaries.

Keywords: Metal Organic Framework, Zeolitic Imidazolate Framework Membrane, Desalination, Forward Osmosis

INTRODUCTION

Production of clean water from saline water resources, such as brackish water and seawater, is an alternative approach to meet clean water demands in an effort to decrease water scarcity [1]. Desalination of saline water, especially for monovalent ions, is always a challenge. Although conventional desalination technologies based on thermal distillation separation, such as multi-stage flash (MSF) and multi-effect distillation (MED), are effective to separate salt, these approaches require a high amount of energy, causing them to be economically inefficient [2]. Compared to these conventional technologies, membrane-based desalination offers a better alternative due to its low energy utilization and lower cost. Reverse osmosis (RO) is a typical membrane process used in desalination as it is able to remove monovalent ions. However, RO still requires additional extra energy in terms of pressure to drive the separation process [3].

This has led to interest in utilizing osmotically driven membrane processes (ODMPs) for desalination, especially forward osmosis (FO). In this process, separation is induced by the difference of osmotic pressure on both sides of the solution across the membrane. This approach enables water to diffuse based on a concentration gradient from low concentration solution (feed) to high concentration solution (draw). Energy consumption in FO is thus lower than RO since no hydraulic pressure is involved, making it more environmental friendly due to minimal energy consumption [4]. In terms of performance, FO has low susceptibility of membrane fouling which will enhance the life span of the membrane without compromising its solute rejection ability [5]. Thus, FO has great potential to become an excellent alternative desalination technology.

Nanostructured materials have also recently gained significant attention for membrane separation applications, particularly in water purifications. Among the array of nanostructured materials, metal organic frameworks (MOFs) are considered as emerging materials due to their exceptional separation properties, e.g., controllable pore sizes, adsorption affinities and high porosity [6,7]. To use MOF as an effective membrane, MOF is deposited onto an inorganic support to provide mechanical strength and chemical resistance during the synthesis and separation process. Typically, research on MOF membranes has focused mainly on gas separation applications, but there is emerging research that has used these materials for water

†To whom correspondence should be addressed.
E-mail: r-mukhlis@utm.my

separation, especially water desalination. Recently, Liu et al. reported UiO-66 ($Zr_6O_4(OH)_4(BDC)_6$) supported on alumina hollow fiber to exhibit high rejection of multivalent ions (99.3% for Al^{3+}, 98.0% for Mg^{2+} and 86.3% for Ca^{2+}) but moderate rejection of monovalent ions (47.0% for Na^+ and 45.7% for K^+) with membrane flux of 1.4 L/m^2·h using dead-end filtration system [8]. They concluded that the MOF membrane is a promising candidate for water desalination by size exclusion due to the ultra-small pore aperture of the MOF.

Various types of MOFs have been synthesized and characterized. However, increasing attention has been given to a subclass of MOFs: the zeolitic imidazolate frameworks (ZIFs) that consist of zinc or cobalt ions coordinated by imidazole-based linker. This MOF family displays a high thermal and chemical stability [9]. Under this group, ZIF-8 is mostly studied for various separation applications [10]. ZIF-8 has a zeolite-like-structure that resembles aluminosilicates zeolite with sodalite (SOD) topology. It has been regarded as a promising membrane material for desalination due to a pore aperture of 0.34 nm, which is larger than the kinetic diameter of H_2O (0.276 nm) but smaller than Na^+ (0.716 nm)/Cl^- (0.664 nm) [11,12]. In addition, ZIF-8 has also been reported to be stable in seawater after exposure to seawater for 15 days without any structural changes, as shown by the XRD analysis [13]. This excellent stability in seawater has enabled ZIF-8 to be used for membrane desalination. However, Duke et al. reported that in a pressurized cross flow filtration system, ZIF-8 membranes showed a poor salt rejection performance [12], where the highest salt rejection was 6% at 7 bar despite an extremely high flux at 600 kg/m^2·h. However, when ZIF-8 membranes were used in pervaporation, the membrane successfully rejected salt as high as 99.8% with water flux of 13.5 kg/m^2·h at 100 °C.

Typically, MOF membranes deposited on porous support were prepared using *in situ* growth or seeded growth. ZIF-8 membranes can be also deposited on a support using the seeded growth method [14,15]. However, this technique may suffer from poor membrane adhesion due to the seed that may weakly adsorb onto the support [16,17]. Preparation of ZIF-8 membranes using *in situ* growth still faces challenges due to poor interaction between the surface of the inert support and the membrane [6]. Therefore, the support will often have to undergo surface modifications to improve nucleation of ZIF-8, which in turn improves the formation of a continuous membrane layer. Various studies have reported the success of synthesizing pure ZIF-8 membranes on an inert support previously deposited with 3-aminopropyltrimethoxysilane (APTES), polydopamine (PDA) and ZnO [16-21]. The deposited ZnO particles acted as a seed to promote the growth of ZIF-8 membrane and anchor to the support surface. Previously, various researchers have adopted different techniques to modify the support with ZnO such as developing composite Al_2O_3/ZnO membrane by introducing ZnO particles in Al_2O_3 dope preparation, coating the support surface with ZnO via magnetron sputtering technique, sol-gel method, chemical vapor deposition method, electrodeposition of composite ZnO/Hmim and manual rubbing of ZnO deposition [16,17,21-25]. In addition, it is interesting to find the presence of difference metal oxides such as NiO as a seed for the ZIF-8 membrane growth. The PDA is a self-polymerized polymer via oxidation process of dopamine which has an adhesive ability to virtually any surfaces [26]. Recently, researchers have developed ZIF-8 membrane on PDA modified support for various application [13,27,28]. Huang et al. reported that PDA provides abundant hydroxyl and amine functional groups on the surface of the support which covalently linked with Zn^{2+} and bind to the ZIF-8 crystals [19].

The presence of sodium formate in synthesis solution is important for the good intergrowth of ZIF-8 membrane. In solvothermal process, sodium formate acts as a deprotonating modulator by deprotonate bridging 2-methylimidazole ligand to drive the crystallization of ZIF-8 [29]. Thus, additional of sodium formate will result in uniform growth of ZIF-8 crystals, which is essential for the preparation of continuous and well-intergrown of ZIF-8 membrane [30]. The amount of sodium formate affected the crystal size, as increase of sodium formate led to smaller crystals as reported by Cravillon et al. [29]. Thus, it is expected the amount of sodium formate in ZIF-8 membrane preparation will affect membrane morphology and performance.

Therefore, we focused on the *in situ* synthesis of ZIF-8 membranes, using the solvothermal process, onto alumina hollow fiber with the presence of ZnO, NiO and PDA. In addition, the different molar ratio of sodium formate in synthesis solution was studied on the membrane characterization and performance. The performance of ZIF-8 membranes in desalination was evaluated using FO. To the best of our knowledge, no studies have reported on ZIF-8 membranes for desalination using FO. As this separation process did not require an external pressure, the ZIF-8 membranes were expected to exhibit an improved performance compared to other MOF membranes tested under the pressure-driven operation.

EXPERIMENTAL WORK

1. Materials

In situ synthesis of ZIF-8 membranes required zinc chloride (97+%, Acros organics), 2-methylimidazole (99%, Acros Organics), sodium formate (ACS Reagent, Acros Organics) and methanol (ACS reagent, Merck). Alumina hollow fiber, used as membrane support, was fabricated using the phase inversion technique. This process required Al_2O_3 powder with the size of 1 μm (99.9%), 0.5 μm (99.5%), 0.01 μm (99.8%) purchased from Alfa Aesar, Arlacel P135 (Uniqema), polyethersulfone (PESf, Radal A300, Ameco Performance), and N-methyl-2-pyrrolidone (AR grade, Qrec) as a solvent. Citric acid (99%, Sigma-Aldrich), ethylene glycol (99.8%, Sigma-Aldrich), metal salt of zinc nitrate hexahydrate ($Zn(NO_3)_2{\cdot}6H_2O$, 98%, Sigma-Aldrich) and nickel (II) nitrate hexahydrate ($Ni(NO_3)_2{\cdot}6H_2O$, 97%, Sigma-Aldrich) were used for the preparation of ZnO and NiO sols, respectively, using the sol-gel Pechini method. Dopamine (99%, Acros Organics) and tris(hydromethyl) aminomethane hydrochloride (Tri-HCl, 99+%, Acros Organics) were used in PDA modification on the surface of alumina hollow fibers.

2. Preparation of Alumina Hollow Fiber

Asymmetric alumina hollow fibers were prepared using the phase inversion technique based on a procedure reported elsewhere [31]. 1.3 wt% of Arlacel was dissolved in a N-methyl-2-pyrrolidone (NMP) solution before the addition of different Al_2O_3 powder loading (53 wt%) at a ratio of 1 : 2 : 7 (0.01 mm : 0.05 mm : 1 mm). Then, the suspension was rolled in a planetary ball milling machine

(NQM-2 Planetary Ball Mill) with different sizes of alumina agate milling balls (20 mm and 10 mm). The rate of the planetary ball milling machine was fixed at 182 rpm for 48 h. Later, a polymer binder at an alumina/PESf ratio of (6 : 1) was added and the milling process was continued for another 48 hr. The alumina suspension was subjected to a vacuum degassing treatment to remove excessive bubbles trapped inside the suspension. The suspension was then extruded into a spinneret before being immersed in a coagulation bath to produce alumina hollow fiber support precursor. To complete the phase inversion process, the alumina precursor was immersed in a water bath for 24 hr. The precursor fibers were then straightened and dried before cut into 35 cm in length. The ceramic precursor was then sintered using a tubular furnace (XL-1700) to obtain alumina hollow fibers supports. The temperature was increased from room temperature to 400 °C at a rate of 3 °C/min and held for 1 h, then to 800 °C at a rate of 4 °C/min and held for 2 h at 1,400 °C before finally held for 8 h at a target temperature rate of 5 °C/min.

3. Surface Modifications of Alumina Hollow Fiber

The deposition of ZnO and NiO onto the outer surface of the alumina hollow fiber was carried out using the sol-gel Pechini method. To prepare ZnO sol, 10.96 g of $Zn(NO_3)_2{\cdot}6H_2O$ was dissolved in 100 ml of deionized (DI) water. After a homogeneous solution was obtained, 14.16 g of citric acid was added into the sol and stirred until fully dissolved. Then, 5.49 g of ethylene glycol was added slowly into the sol while being continuously stirred to ensure well dispersion of ethylene glycol. The sol was stirred for another 24 h to obtain a homogeneous sol. For the preparation of NiO sol, a similar method was used, but nickel (II) nitrate hexahydrate was used as the metal nitrate instead. 11.63 g of $Ni(NO_3)_2{\cdot}6H_2O$, 15.37 g of citric acid and 5.96 g of ethylene glycol were dissolved in 100 ml DI water used to prepare NiO sol. Prior to the deposition process, both ends of the alumina hollow fiber were wrapped with polytetrafluoroethylene (PTFE) tape to avoid metal oxides being deposited inside the hollow fiber. Several alumina hollow fibers were immersed in the Zn sol and Ni sol in separate beakers before being dried in an oven at 120 °C for 24 h. After the drying process, the PTFE tape was removed and the fibers were calcined in a muffle furnace at 400 °C at 5 °C/min heating rate for 1 h.

Surface modification using polydopamine was carried out using a procedure reported elsewhere [13,19,32]. Tris-HCl was dissolved into DI water to prepare 10 mM of Tris-HCl buffer solution (pH: 8.5). Then, 2 mg of dopamine hydrochloride was added in each ml of 10 mM of Tris-HCl buffer in an open glass vial. Prior to the polydopamine coating process, both ends of the alumina hollow fiber were wrapped with PTFE tape to ensure polydopamine coating occurs only on the outer surface of the alumina hollow fiber. The alumina hollow fiber was then treated with the dopamine solution at 20 °C and stirred for 20 h, leading to the polymerization of the polydopamine (PDA) layer onto the surface of the alumina hollow fiber. The PDA-modified hollow fiber was then rinsed using ultra-pure water to remove excess PDA before dried in an oven at 60 °C for 24 h. Surface modification for PDA deposition was carried out once without seed re-deposition.

4. Synthesis of ZIF-8 on Modified Alumina Hollow Fiber

ZIF-8 membranes were synthesized on modified alumina hollow fibers using the *in situ* growth method via solvothermal process. In a typical synthesis procedure, zinc chloride, 2-methylimidazole (Hmim) and sodium formate (SF) were dissolved in methanol (MeOH). The molar ratio of synthesis solution that consisted of $ZnCl_2$, Hmim, SF and MeOH was fixed at 1 : 2 : 1 : 313, respectively, adopting the formulation studied by Liu et al. [27]. This formulation was labeled as SF-1. To study the effect of sodium format on the formation of ZIF-8, the ratio of sodium formate was increased to 2, while other compositions remained constant. This formulation was known as SF-2. Both ends of the alumina hollow fiber were wrapped with PTFE to avoid the synthesis solution from entering the lumens prior to the synthesis process. The synthesis solution was filled into a Teflon bottle, which contained the modified alumina hollow fibers, and later heated at 60 °C in an oven for 24 h. When the solvothermal process was completed, the ZIF-8 membranes were cooled to room temperature before being washed several times with methanol to remove loosened ZIF-8 powder on the surface of the membranes and then dried under room temperature for 24 h.

5. Characterizations

Crystallinity of the ZIF-8 powder was determined by X-ray diffraction (XRD) using Siemens X-ray diffractometer D5000 with Cu Kα radiation. The step speed of 2°/min and 2θ degrees ranging from 5° to 40° were used to record XRD patterns of the sample. The XRD patterns of ZnO and NiO seeds obtained from the sol-gel Pechini method were recorded using the same equipment with 2θ degrees ranging from 30° to 80°. Fourier transform infrared (FT-IR) analysis was used to determine the presence of PDA on the alumina hollow fiber. FTIR spectra were recorded using Shimadzu IRTracer-100 operating in absorbance mode. The surface morphology and thickness of both ZIF-8 and alumina hollow fiber membranes were observed using the field-emission scanning electron microscopy (FESEM) taken by ZEISS Crossbeam 340.

6. Evaluation of Membrane Performance in FO System

The performance of ZIF-8 membranes in desalination was studied using a cross-flow lab-scale FO system as shown in Fig. 1. In this system, two peristaltic pumps (NE-9000, New Era Pump Systems, USA) were used to flow the draw and feed solutions. In a typical FO test, the feed solution was introduced on an active layer of ZIF-8 membrane, whereas the draw solution was flowed in the lumen of the hollow fiber. This configuration is known as 'an active layer face feed solution' (AL-facing FS). The flow rate of the feed and draw solutions was fixed at a flow rate of 250 ml/min and 130 ml/min, respectively. An electronic balance (LT1002E, Changsu TianLiang Instrument, China) was used to measure weight changes of the feed solution during the testing.

To determine water flux, DI water was used as the feed solution, whereas 100,000 ppm (1.7 M) of NaCl was used as the draw solution. The duration of testing was kept constant at 1 h. The water flux (Jw) was measured during the separation process and calculated based on formula 1.

$$Jw = \frac{\Delta m}{A\Delta t} \quad (1)$$

where Δm is the weight change of the draw solution, A is the area of the effective membrane, and Δt is experimental time.

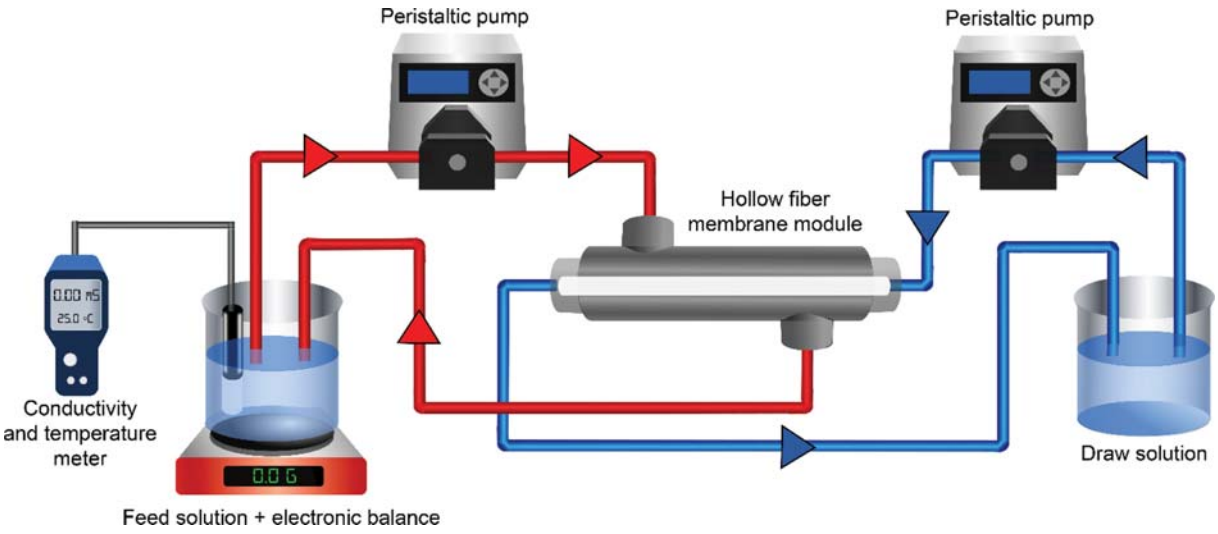

Fig. 1. FO permeation set-up to study the performance of ZIF-8 membranes.

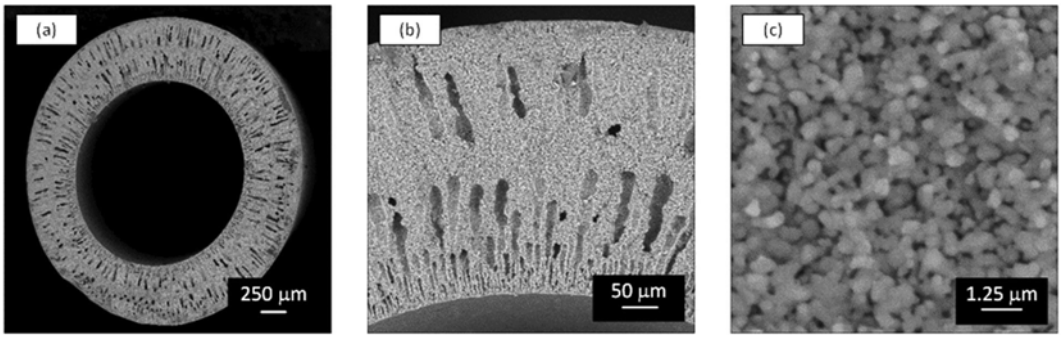

Fig. 2. SEM images of alumina hollow fiber support by (a) cross section, (b) enlarged cross section, and (c) outer surface.

To determine the reverse solute flux from the draw solution to the feed solution across the membrane, conductivity of the feed solution, which contained DI water, was measured using the conductivity meter before and after testing. Concentrations of salt in the feed solution were calculated from the conductivity values using a calibration curve. The reverse solute flux (Js) was computed using formula 2 [4]:

$$Js = \frac{\Delta(C_t V_t)}{A\Delta t} \quad (2)$$

where C_t is the concentration of salt of the feed solution, while V_t is the volume of the feed solution, and Δt is experimental time.

A similar permeation set-up was used to measure the salt rejection (R) of the ZIF-8 membrane. In this procedure, 0.1 M NaCl and 1.0 M dextrose were used as the feed and draw solution, respectively. The salt rejection, (R) was calculated using Eq. (3) [4]:

$$R = \left(1 - \frac{C_p}{C_f}\right) \times 100\% \quad (3)$$

where C_p is the permeate concentration calculated from the quantity of salt and water transfer from the feed to draw solution. C_f is the initial concentration of salt of the feed solution.

RESULTS AND DISCUSSION

1. Morphology of Alumina Hollow Fiber Support

Fig. 2 shows the morphology of the alumina hollow fiber prepared using the phase inversion and sintering technique. Using this technique, the asymmetric structure of an inert support was formed, consisting of a sponge-like region in the middle of a finger-like structure that originated from both the lumen and shell side to form a sandwich-like structure. The formation of the finger-like structure was due to a slow solvent/non-solvent exchange from the ceramic suspension to the coagulation bath [33]. The alumina hollow fiber, used as an inert support for the ZIF-8 membrane, had outer and inner diameters of 1.63 mm and 1.08 mm, respectively, with a thickness of 0.26 mm. The support had a smooth outer surface with a surface roughness of 37.5 nm. Therefore, an intermediate layer on top of the ceramic hollow fiber was not a priority. The hollow fiber had excellent porosity, which enabled high pure water flux at 519.34 L/m^2·h in a cross-flow filtration system.

2. Synthesis and Characterization of ZIF-8

Fig. 3 shows the XRD spectra of the ZIF-8 particles collected from a Teflon bottle after *in situ* synthesis of alumina hollow fibers. The peaks in both XRD spectra are well matched with the simulated structural data of ZIF-8. The results indicated that highly crys-

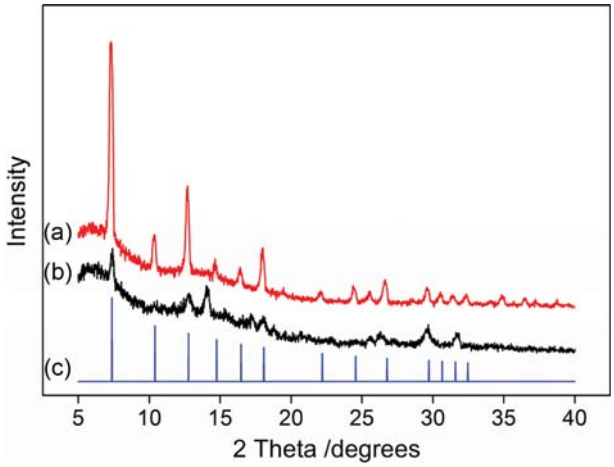

Fig. 3. XRD patterns of ZIF-8 powder from (a) SF-1, (b) SF-2 synthesis solution and (c) simulated data [9].

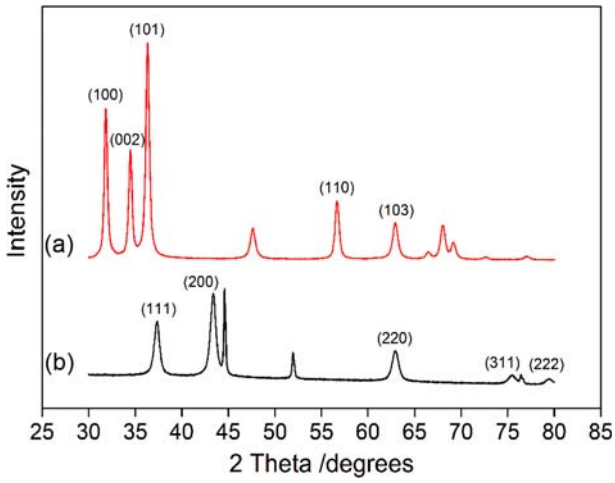

Fig. 4. XRD pattern of (a) ZnO and (b) NiO seed from sol-gel Pechini method.

talline ZIF-8 particles were successfully obtained from both SF-1 and SF-2 synthesis solutions. It can be seen that ZIF-8 prepared using a synthesis solution of SF-1 produced sharper peaks compared to SF-2, which showed slightly broader peaks. Thus, this indicates that the crystal grains of ZIF-8 particles made from SF-2 were larger than those formulated from SF-1 based on Scherrer's equation.

In this study, the outer surface of the alumina hollow fibers was deposited with ZnO and NiO particles, using the sol-gel Pechini method, and PDA to improve the growth of ZIF-8 membrane. Preparation of ZIF-8 membranes by *in situ* growth without surface modification has been shown to cause the formation of membranes with poor performance, as reported by [16,19]. Therefore, metal oxides were used as a seed or template in promoting crystallization of MOFs on the alumina hollow fiber. The deposition of metal oxides onto the alumina hollow fiber occurred by surface interaction due to surface hydroxyl group present on both seeds and the support. This finding has been discussed by Garcia et al [34]. In the case of ZIF-8, ZnO was typically used to prepare a well-intergrown and continuous membrane. This is because ZnO promotes the formation of ZIF-8 crystals by generating a large number of nucleation sites, as zinc from bulk ZnO saturated on the support reacts with the ligand [25]. To study the ability of other metal oxides to promote ZIF-8 growth, NiO was deployed as a seed for the preparation of ZIF-8 membranes. Besides that, PDA, which is a linker, had also been used in this work to link ZIF-8 crystals covalently on the surface of the support, to form a dense membrane.

The XRD analysis, as shown in Fig. 4, showed that ZnO and NiO seeds were successfully synthesized from the sol-gel Pechini method. In Fig. 4(a), the sharp diffraction peaks from as-prepared ZnO at 2θ of 31.8, 34.4, 36.2, 56.6 and 62.8° were identified as the (100), (002), (101), (110) and (103) crystal planes of ZnO, respectively, which is in agreement with the standard values (ICDD 01-079-5604). For as-prepared NiO, peaks at 2θ of 37.2, 43.2, 62.8, 75.5, 79.3° can be associated as the (111), (200), (220), (311), and (222) crystal planes, respectively (Fig. 4(b)), are well matched with the standard values of NiO (ICDD 01-078-0643). Furthermore,

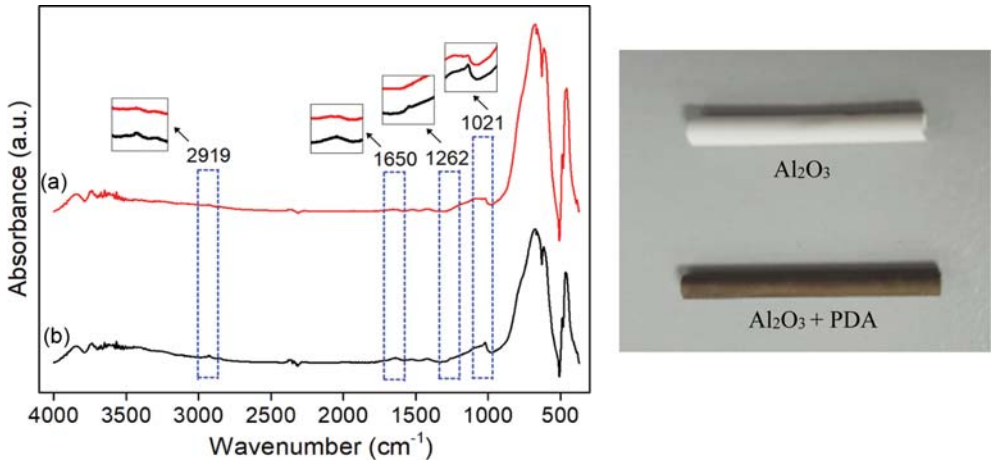

Fig. 5. FTIR spectra of (a) bare alumina hollow fiber and (b) PDA-modified alumina hollow fiber.

well-defined diffraction peaks indicate the formation of high crystallinity and high quality of as-prepared ZnO and NiO.

PDA was polymerized on the surface of alumina hollow fiber. Initial observations showed that the white appearance of alumina hollow fiber turned to dark brown after PDA modifications. This indicates that PDA had been deposited on the surface of the support, as shown in Fig. 5, which is similar to the observations made by Zhou et al. and Wei et al. [32,35]. Based on Lee et al. [26], PDA

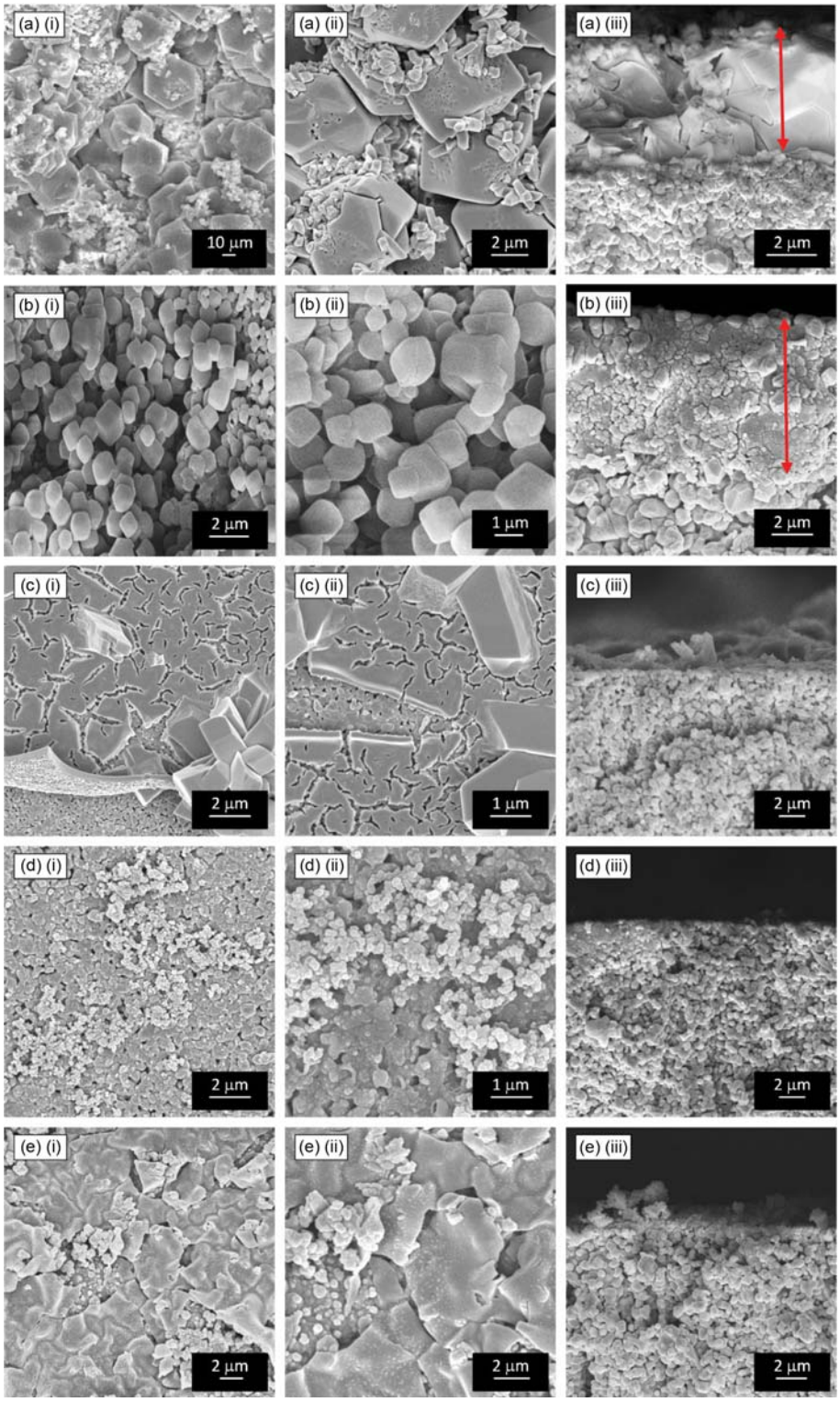

Fig. 6. FESEM images of (a) ZnO/ZIF-8 (SF-1), (b) ZnO/ZIF-8 (SF-2), (c) NiO/ZIF-8, (d) PDA/ZIF-8 and (e) PDA/ZIF-8 (regrowth) membranes for the (i) surface, (ii) magnified surface and (iii) cross-section.

was deposited by self-polymerization through oxidation process, in which interact covalent and non-covalently with the surface of the support. The presence of PDA on the alumina hollow fiber was confirmed by comparing FTIR spectra of bare alumina hollow fiber and PDA-modified alumina hollow fiber. From Fig. 5, the FTIR spectrum for PDA-modified alumina hollow fiber showed weak absorbance peaks at bands 1,021 cm^{-1}, 1,262 cm^{-1}, 1,650 cm^{-1} and 2,919 cm^{-1}. This is expected as intensities of the FTIR peaks were influenced by the amount of PDA deposited on the alumina hollow fiber. Additionally, this result is similar to the work reported by Zhou et al. who analyzed the deposition of PDA on alumina tubes [32]. The presence of band 1,021 cm^{-1} can be assigned to C-O vibration, and band 1,262 cm^{-1} can be associated with C-OH vibration. The bands at 1,650 cm^{-1} and 2,919 cm^{-1} can be assigned to N-H (amide) and C-H vibrations, respectively [36].

Supported ZIF-8 membranes were synthesized *in situ* on alumina hollow fiber using the solvothermal process at 60 °C for 24 hr. Fig. 6 shows the FESEM images of ZIF-8 membranes prepared using SF-1 and SF-2 synthesis solutions, on the outer surface of alumina hollow fiber with different surface modifications. As demonstrated in Fig. 6(a) (i) and (ii), the surface of the ZnO/ZIF-8 (SF-1) membrane was completely covered with the ZIF-8 membrane. From the cross-section view shown in Fig. 6(a) (iii), it was shown that a well-defined ZIF-8 membrane has been formed with a thickness of 6 μm, consisting of smaller and larger ZIF-8 crystals. Smaller ZIF-8 crystals adhered to the surface of the larger ZIF-8 crystals, with the latter deposited on the surface of the alumina hollow fiber. The formation of uneven ZIF-8 crystals suggested that the crystals did not fully undergo nucleation to achieve a stable equilibrium ZIF-8 morphology, from the cubic to rhombic dodecahedron shape, even after 24 h of synthesis. As reported by Cravillon et al., a combination of smaller and larger ZIF-8 crystals can only be seen at the early synthesis period, as later on the smaller crystals will grow into large crystals assuming the shape of rhombic dodecahedron [29]. ZnO particles deposited onto the alumina hollow fiber acted as a secondary source of zinc to react with Hmim ligand as an anchor for ZIF-8 crystals to form a membrane on the outer surface of the alumina hollow fiber [25]. The use of ZnO seed, synthesized using the sol-gel technique for the preparation of ZIF-8 had been previously reported by Zhang [16], which is con-

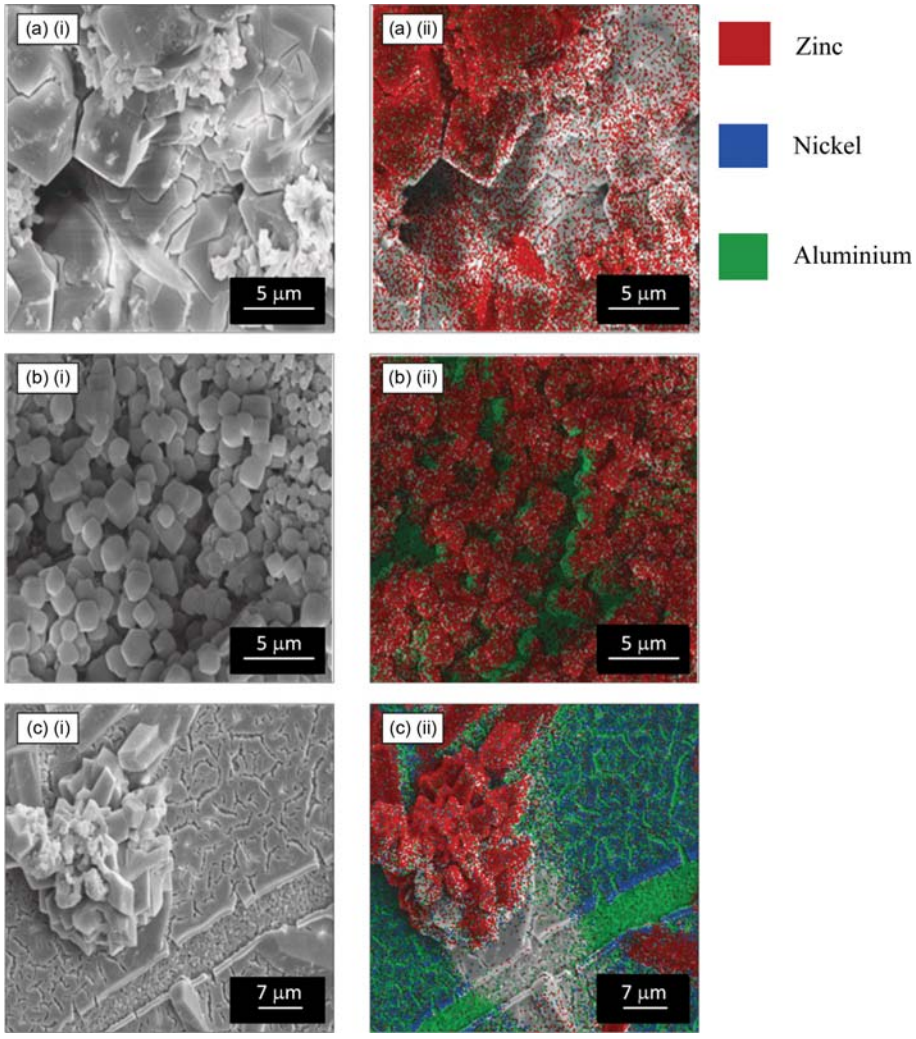

Fig. 7. FESEM and EDX images of (a) ZnO/ZIF-8 (SF-1), (b) ZnO/ZIF-8 (SF-2) and (c) NiO/ZIF-8 membranes.

sistent with our observation.

Fig. 6(b) shows the FESEM images from the top-view and cross-sectional view of the ZnO/ZIF-8 membrane, synthesized using SF-2 synthesis solution. The images showed the support to be fully covered by a uniform layer of ZIF-8 crystals. As a result, ZIF-8 membrane with thickness of 8.5 μm was formed. It can also be seen that the crystals of the ZIF-8 membrane resemble a cubic shape. An increase in SF molar ratio from 1 to 2 caused the size of the ZIF-8 crystals to become smaller, which is in agreement with the XRD analysis. SF acted as a modulator where its function is to deprotonate the bridge between Hmim ligands with Zn^{2+}, increasing the amount of SF resulting in smaller ZIF-8 crystals to grow due to accelerated nucleation of a larger number of nuclei [29,37]. This contributed to an increase in the membrane thickness as the crystals were closely packed together to form the ZIF-8 membrane. Fig. 7(a) and 7(b) shows the FESEM-EDX of ZnO/ZIF-8 (SF-1) and (SF-2), respectively. From the element mapping, aluminium element was detected in the surface for both membranes. However, the mapping intensity for ZnO/ZIF-8 (SF-2) was higher than of (SF-1), which is represented by green color. By increasing SF molar ratio from 1 to 2, the deposition of ZIF-8 membrane became poorer. High amount of SF was predicted to hamper the ZIF-8 crystals growth and retard its nucleation [38].

The FESEM analysis on the ZIF-8 membrane, which used NiO particles as seeds, prepared using the SF-1 synthesis solution is shown in Fig. 6(c). The ZIF-8 membrane is seen to grow directly onto the alumina hollow fiber in clusters. The shape of the ZIF-8 crystals is rectangular, which completely differs from the shapes of the ZIF-8 crystals displayed in Fig. 6(a) and Fig. 6(b). Furthermore, ZIF-8 membranes that were synthesized using NiO particles as seeds suffered from severe delamination. Fig. 7(c) shows the FESEM-EDX mapping of the ZIF-8 membrane that differentiated elements in the membrane, seed and support. Poor deposition of ZIF-8 on the alumina hollow fiber suggested that NiO did not promote surface nucleation of ZIF-8, although zinc and nickel have similar ionic charges. This is because Ni^{2+} did not react with Hmim ligands in the same manner as its reaction to Zn^{2+} in creating an active site for ZIF-8. Based on this finding, it can be concluded that the seed should have a similar metallic element to the metal ion used in synthesizing MOF to induce crystal growth on porous supports.

When *in situ* solvothermal synthesis was carried out on alumina hollow fiber consisting of PDA, the surface of the support was unexpectedly not covered with a ZIF-8 layer as the crystal growth was isolated and scattered, as shown in Fig. 6(d) (i) and (ii). The crystals were smaller even when compared to the ZIF-8 crystals using the SF-2 synthesis solution, although similar synthesis conditions were used for all membrane samples. As a result, no membrane layer was found when FESEM analysis was carried out on the cross-sectional of the alumina hollow fiber, as shown in Fig. 6(d) (iii). This study was unable to demonstrate that PDA could be used to promote well-intergrown ZIF-8 membranes as previously reported [13,19]. This result could be due to a limited amount of amine and hydroxyl groups on the alumina hollow fiber after the deposition of PDA, as shown in Fig. 5. These groups are responsible to react covalently with Zn^{2+} ions from zinc precursor to form a continuous ZIF-8 membrane on the surface of the support [19].

Table 1. Water contact angle measurement

Membrane type	Contact angle
ZnO/ZIF-8 (SF-1)	64.14±4.31°
ZnO/ZIF-8 (SF-2)	63.27±10.05°
NiO/ZIF-8	54.73±1.44°
PDA/ZIF-8	32.59±2.71°
PDA/ZIF-8 (re-deposition)	45.41±4.00°
Pristine alumina hollow fiber	30.72±11.92°
ZIF-8 [39]	92°

The ZIF-8 crystals deposited on the PDA modified surface resembled seed particles for secondary growth, as reported by [14] who prepared ZIF-8 hollow fiber membranes by secondary growth. The re-deposition of ZIF-8 membrane was carried out using similar synthesis solution (SF-1) and synthesis conditions. This process enabled a thin ZIF-8 membrane to be formed despite some uncovered areas as shown in Fig. 6(e). There were visible cracks on the ZIF-8 membrane, resulting in a non-continuous layer. This result can be explained by the fact that the PDA layer was present in a small quantity on the outer surface of the alumina hollow fiber. This was proved by FTIR analysis, although the peaks that represented PDA can be observed, but low concentration of PDA caused low intensity of the FTIR peaks. A small amount of this polymer caused the formation of small ZIF-8 crystals at scattered locations. Re-deposition of ZIF-8 was ineffective as it led to an uneven growth of ZIF-8 layer on the seeds, resulting in the formation of membrane defects.

Table 1 shows the water contact angle of the membranes. The water contact angle of all synthesized membranes was higher than that of pristine alumina hollow fiber due to the deposition of ZIF-8, which is a hydrophobic material. Both ZnO/ZIF-8 (SF-1) and (SF-2) have the highest water contact angle followed by NiO/ZIF-8, PDA/ZIF-8 (re-deposition) and PDA/ZIF-8 at the angle of 64.14±4.31°, 63.27±10.05°, 54.73±1.44°, 45.41±4.00° and 32.59±2.71°, respectively. The lower water contact angle for NiO/ZIF-8, PDA/ZIF-8 and PDA/ZIF-8 (re-deposition) membranes indicates the poor deposition of ZIF-8 crystals, in an agreement with FESEM analysis earlier. Compared to water contact angle from reference at 92°, both ZnO/ZIF-8 membranes have lower water contact angle. This can be associated to the formation of thin ZIF-8 layer on alumina hollow fiber causing water in contact with the surface of the support during the measurement which. This was in agreement with the result in Fig. 7 that the aluminium element be detected using FESEM-EDX analysis. The re-deposition of ZIF-8 should be carried out to minimize defect.

3. FO Performance of ZIF-8 Membranes for Desalination

To evaluate the performance of ZIF-8 membranes in terms of water flux and reverse solute flux in FO system, distilled water was used as a feed solution, whereas 1.7 M NaCl solution was used as the draw solution. The draw solution was introduced into the lumen of the alumina hollow fiber, while the feed solution was introduced on the outer surface of the ZIF-8 membrane. The FO concept used the osmosis phenomenon, resulting in water to migrate from a

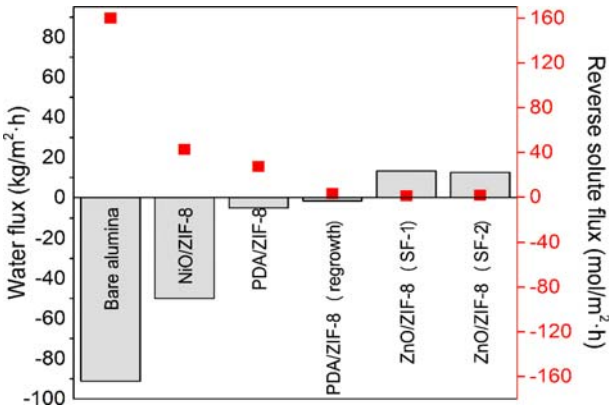

Fig. 8. Water flux and reverse solute flux of prepared ZIF-8 membranes and bare alumina membrane. The draw solution was 100,000 ppm (1.7 M) NaCl solution, and DI water was chosen as feed solution.

low concentration to a high concentration. To confirm the performance of the ZIF-8 membranes, pristine alumina hollow fiber was used as a control. Fig. 8 shows the water fluxes and reverse solute fluxes of the ZIF-8 membrane and pristine alumina hollow fiber. The ZnO/ZIF-8 membranes synthesized using SF-1 and SF-2 synthesis solutions exhibited water fluxes as high as 13.3 kg/m^2·h and 12.5 kg/m^2·h, respectively. On the contrary, reverse solute flux for ZnO/ZIF-8 membrane (SF-1) was slightly lower (0.95 mol/m^2·h) than ZnO/ZIF-8 (SF-2) at 1.64 mol/m^2·h. The difference in water flux between SF-1 and SF-2 can be associated with the membrane's thickness. Thick membranes typically increase resistance and restrict water pathway across the membrane.

The water flux results for both membranes are comparable to the pervaporation results reported by Zhu et al. [13]. The authors reported their ZIF-8 membrane to display a water flux as high as 13.5 kg/m^2·h at 100 °C through pervaporation. ZnO/ZIF-8 membranes in this study exhibited a relatively higher water flux compared to commercial cellulose acetate (CA) (~8 kg/m^2·h) and comparable to commercial thin-film composite (TFC) (~15 kg/m^2·h) membranes from Hydration Technology Inc. (HTI). However, the as-prepared membrane displayed much higher reverse solute fluxes compared to both HTI membranes (CA at ~0.01 mol/m^2·h and TFC at 0.07 mol/m^2·h) using 1 M NaCl draw and DI water feed solution [40]. High water flux is associated with the presence of non-polar groups (CH_3) in ZIF-8, resulting in hydrophobic framework with low affinity towards water molecules. Gupta et al. demonstrated that hydrophobic/non-polar ZIF produced higher water permeance compared to hydrophilic/polar ZIFs, as water strongly bound into the hydrophilic framework reduces water flow [41]. They concluded that water flux was dependent on ZIFs' functional group polarity rather than its pore size. Both ZIF-8 membranes were subjected to salt rejection studies to predict any defect occurrence on the ZIF-8 layer since the reverse solute fluxes were relatively high.

When NiO and PDA were used as seeds, ZIF-8 membranes exhibited negative water fluxes. Negative water flux is an undesirable condition, as it involves the diffusion of the draw solution to the feed solution, halting the osmosis phenomenon through a semi-permeable membrane. FESEM and FESEM-EDX analysis has shown the membranes had severe cracks that cause exhibited negative water fluxes. NiO-ZIF-8 and PDA-ZIF-8 membranes have water fluxes of −50 kg/m$_2$·h and −5.2 kg/m$_2$·h, respectively. There was a slight improvement in the water flux of the PDA-ZIF-8 membrane after the re-deposition process, despite the membrane exhibiting a negative flux of −1.7 kg/m$_2$·h. These results are consistent with the ones produced by the pristine alumina hollow fiber that exhibited the highest negative flux of −91.14 kg/m^2·h. As the pristine alumina hollow fiber did not have a selective membrane on its outer surface, it could not retain the solute in the draw solution from passing through into feed solution, resulting in poor separation performance.

The permeation of solutes for both NiO/ZIF-8 and PDA/ZIF-8 membranes from the draw solution to the feed solution was further evaluated using their reverse solute fluxes. From Fig. 8, the pristine alumina hollow fiber had the highest reverse solute flux of 160.9 mol/m^2·h, followed by NiO/ZIF-8 membrane (42.66 mol/m^2·h), PDA/ZIF-8 membrane (27.42 mol/m^2·h) and the PDA/ZIF-8 membrane subjected to the re-deposition process (3.22 mol/m^2·h). The trend was similar to the water flux, showing that an increase in the flow rate of the feed solution was caused by solute penetration into the feed solution. Thus, it can be concluded that the membranes were not suitable for desalination.

Efficiency of the ZnO/ZIF-8 membranes in rejecting salt was determined using the FO system. 0.1 M NaCl and 1 M dextrose were used as the feed and draw solutions, respectively. This study was to confirm the high reverse solute fluxes of ZnO/ZIF-8 for both the SF-1 and SF-2 synthesis solutions. In this measurement, salt rejection was measured based on the forward solute flux from the feed solution to the draw solution. Fig. 9 shows that the ZnO/ZIF-8 membrane, synthesized using the SF-2 synthesis solution, exhibited 54.9% salt rejection, slightly higher compared to 52.1% salt rejection obtained using ZnO/ZIF-8 membrane, synthesized using SF-2 synthesis solution. However, this finding was still far from achieving the theoretical performance of ZIF-8 for the desalina-

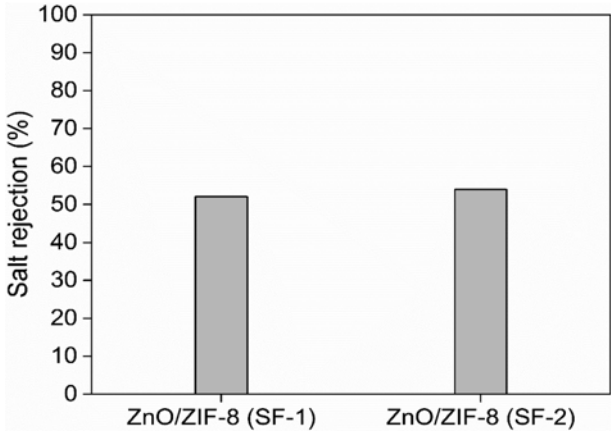

Fig. 9. Salt rejection of ZnO/ZIF-8 (SF-1) and ZnO/ZIF-8 (SF-2) membranes. The draw solution was 1.0 M dextrose solution and feed solution was 0.1 M NaCl solution.

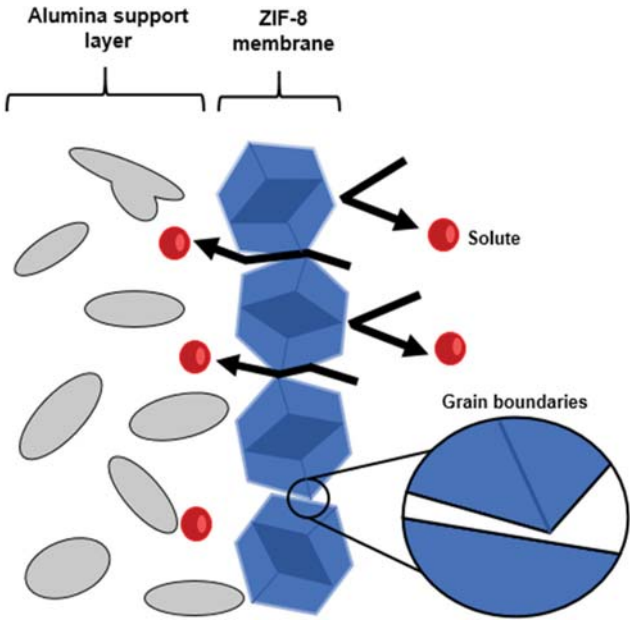

Fig. 10. Conceptual mechanism of solute pathway in the presence of grain boundaries.

tion process. As reported by Hu et al., a simulation study predicting the performance of ZIF-8 membranes for RO desalination should obtain 100% salt rejection, as Na^+ and Cl^- ions cannot pass across the membrane [42]. Lower salt rejection of ZnO/ZIF-8 membranes suggested that the membrane had some sort of defect or flexible pore aperture [43] or combination of both that can reduce the membrane selectivity. The most likely defect to occur in ZIF-8 membranes is the formation of grain boundaries between ZIF-8 crystals. The main reason for moderate salt rejection can be associated with the presence of grain boundaries which results in non-continuous membrane as previously shown in FESEM images (Fig. 6). Grain boundaries are known as surface imperfections in polycrystalline materials that separate grains of different orientations. These defects allow the solute to pass across the membrane easily as depicted in Fig. 10. As ZIF-8 is categorized as a crystalline material, it is impossible to avoid the formation of this defect. However, the number of defects in the material can be minimized by allowing the crystal to grow bigger.

The salt rejection of ZnO/ZIF-8 membranes obtained in this work was higher compared to the ZIF-8 membrane developed by Duke et al. [12]. The membrane allowed salt rejection of up to 6.3% using a pressurized system. This trend could be correlated with the separation process using forward osmosis, performed at ambient pressure, while keeping the structure of the ZIF-8 membrane intact. As reported by Duke et al., the reason for poor RO desalination performance of ZIF-8 membranes was due to the loss of Zn^{2+} from the ZIF-8 framework [12]. They also reported that when feed pressure was increased from 150 kPa to 200 kPa, the salt rejection decreased from 6.3% to 0%. This suggested that loss of Zn^{2+} can be associated with a high-pressure system, indicating that ZIF-8 membranes should be used in FO, which clearly offers better results compared to if used in RO.

CONCLUSION

We developed ZIF-8 membrane on alumina hollow fiber for desalination application using in-situ growth by solvothermal process. In the membrane preparation process, the support was deposited with ZnO, NiO and PDA to study the effect of different surface modification seed. From XRD analysis, we successfully synthesized ZIF-8 in both SF-1 and SF-2 synthesis solution. Proved by FESEM analysis, there was no continuous and dense ZIF-8 membrane formed for PDA/ZIF-8, PDA/ZIF-8 (re-deposition) and NiO/ZIF-8 membrane. The ZIF-8 crystal appeared scattered on PDA modified support. Even though the ZIF-8 thin layer was formed after re-deposition, the layer suffered from cracks. The FTIR analysis on PDA modified support showed weak absorbance peaks that represented PDA, especially for hydroxyl group vibration, which was responsible for the attachment of ZIF-8 with the support. Weak intensities of PDA peaks indicate low concentration of PDA deposited. The NiO/ZIF-8 membrane suffered from severe crack and delamination of NiO layer as well as formation of islands of ZIF-8 crystal. Introduction of foreign metal oxide such as NiO did not promote the nucleation of ZIF-8. However, only ZnO/ZIF-8 modified support showed a well-defined pure phase ZIF-8 membrane. This is attributed to zinc oxide as a secondary source to react with Hmim ligand, allowing ZIF-8 membrane to be anchored to the support surface. By increasing the molar ratio of SF, the size of ZIF-8 crystals was reduced, resulting in an increase in membrane thickness. The PDA/ZIF-8, PDA/ZIF-8 (re-deposition) and NiO/ZIF-8 membranes exhibited negative water flux of −50 $kg/m^2 \cdot h$, −5.2 $kg/m^2 \cdot h$ and −1.7 $kg/m^2 \cdot h$ with reverse solute flux of 42.66 $mol/m^2 \cdot h$, 27.42 $mol/m^2 \cdot h$ and 3.22 $mol/m^2 \cdot h$, respectively. High reverse solute indicates the membranes were unable to retain the solute from draw solution diffused into the feed solution. ZnO/ZIF-8 (SF-1) membrane managed to achieve water flux of up to 13.3 $kg/m^2 \cdot h$ and reverse solute flux 0.95 $mol/m^2 \cdot h$, while ZnO/ZIF-8 (SF-2) exhibited water flux 12.5 $kg/m^2 \cdot h$ with higher reverse solute flux 1.64 $mol/m^2 \cdot h$. The ZnO/ZIF-8 (SF-1) and (SF-2) displayed a moderate salt rejection at 52.1% and 54.9%, respectively. Moderate ion rejection was attributed to grain boundaries defect, allowing Na^+ and Cl^- ions to pass across the membrane through poor ZIF-8 crystal grains. As a consequence, we found ZIF-8 to be a promising membrane material for desalination by FO. However, improvements in membrane morphology to prepare a well-intergrown, continuous and thin membrane are needed to improve the performance in terms of water flux, reverse solute flux and salt rejection.

ACKNOWLEDGEMENTS

The authors gratefully acknowledge financial support from the Malaysia Ministry of Higher Education (MOHE) through FRGS (0. J130000.7823.4F947), the Higher Institution Centre of Excellence (HICoE) Research Grant (R. J090301.7846.4J176), and Universiti Teknologi Malaysia (UTM) through the Research University grant (Q. J130000.2546.16H34, Q.J130000.2446.04G30). Appreciation also goes to UTM Research Management Centre for both financial and technical support.

REFERENCES

1. K. Wang, A. A. Abdalla, M. A. Khaleel, N. Hilal and M. K. Khraisheh, *Desalination*, **401**, 190 (2017).
2. H. Balfaqih, M. T. Al-Nory, Z. M. Nopiah and N. Saibani, *Desalination*, **406**, 2 (2016).
3. P. S. Goh, T. Matsuura, A. F. Ismail and N. Hilal, *Desalination*, **391**, 43 (2016).
4. E. Yang, C. M. Kim, J.-h. Song, H. Ki, M. H. Ham and I. S. Kim, *Carbon*, **117**, 293 (2017).
5. D. L. Shaffer, J. R. Werber, H. Jaramillo, S. Lin and M. Elimelech, *Desalination*, **356**, 271 (2015).
6. S. Qiu, M. Xue and G. Zhu, *Chem. Soc. Rev.*, **43**, 6116 (2014).
7. M. Lismont, L. Dreesen and S. Wuttke, *Adv. Funct. Mater.*, **27**, 1 (2017).
8. X. Liu, N. K. Demir, Z. Wu and K. Li, *J. Am. Chem. Soc.*, **137**, 6999 (2015).
9. K. S. Park, Z. Ni, A. P. Côte, J. Y. Choi, R. Huang, F. J. Uribe-Romo, H. K. Chae, M. O'Keeffe and O. M. Yaghi, *Proc. Natl. Acad Sci.*, **103**, 10186 (2006)
10. C. Zhang and W. J. Koros, *J. Phys. Chem. Lett.*, **6**, 3841 (2015).
11. Y. Lee, M. Jang, H. Cho, H. Kwon, S. Kim and W. Ahn, *Chem. Eng. J.*, **271**, 276 (2015).
12. M. C. Duke, B. Zhu, C. M. Doherty, M. R. Hill, A. J. Hill and M. A. Carreon, *Desalination*, **377**, 128 (2016).
13. Y. Zhu, K. M. Gupta, Q. Liu, J. Jiang, J. Caro and A. Huang, *Desalination*, **385**, 75 (2016).
14. Y. Pan, B. Wang and Z. Lai, *J. Membr. Sci.*, **421-422**, 292 (2012).
15. H. Bux, A. Feldho, J. Cravillon, M. Wiebcke, Y. Li and J. Caro, *Chem. Mater.*, **23**, 2262 (2011).
16. X. Zhang, Y. Liu, L. Kong, H. Liu, J. Qiu, W. Han and L.-T. Weng, *J. Mater. Chem. A*, **1**, 10635 (2013).
17. L. Kong, X. Zhang, H. Liu and J. Qiu, *J. Membr. Sci.*, **490**, 354 (2015).
18. L. Kong, G. Zhang, H. Liu and X. Zhang, *Mater. Lett.*, **141**, 344 (2015).
19. A. Huang, Q. Liu, N. Wang and J. Caro, *J. Mater. Chem. A*, **2**, 8246 (2014).
20. M. Drobek, M. Bechelany, C. Vallicari, A. A. Chaaya, C. Charmette, C. Salvador-levehang, P. Miele and A. Julbe, *J. Membr. Sci.*, **475**, 39 (2015).
21. X. Wang, M. Sun, B. Meng, X. Tan, J. Liu, S. Wang and S. Liu, *Chem. Commun.*, **52**, 13448 (2016).
22. P. Neelakanda, E. Barankova and K. V. Peinemann, *Micropor. Mesopor. Mater.*, **220**, 215 (2016).
23. M. Wu, H. Ye, F. Zhao and B. Zeng, *Sci. Rep.*, **7**, 1 (2017).
24. I. Stassen, M. Styles, G. Grenci, H. Van Gorp, W. Vanderlinden, S. De Feyter, P. Falcaro, D. De Vos, P. Vereecken and R. Ameloot, *Nat. Mater.*, **15**, 304 (2016).
25. J. Yang, Z. Xie, H. Yin, J. Wang, J. Xu, J. Wang, J. Lu, D. Yin and Y. Zhang, *Micropor. Mesopor. Mater.*, **198**, 263 (2014).
26. H. Lee, S. M. Dellatore, W. M. Miller and P. B. Messersmith, *Science*, **318**, 426 (2007).
27. Q. Liu, N. Wang, R. Caro and A. Huang, *J. Am. Chem. Soc.*, **135**, 17679 (2013).
28. A. Huang, Q. Liu, N. Wang, Y. Zhu and J. Caro, *J. Am. Chem. Soc.*, **136**, 14686 (2014).
29. J. Cravillon, C. A. Schroder, H. Bux, A. A. Rothkirch, J. Caro and M. Wiebcke, *CrystEngComm*, **14**, 492 (2012).
30. M. Shah, H. T. Kwon, V. Tran, S. Sachdeva and H. K. Jeong, *Micropor. Mesopor. Mater.*, **165**, 63 (2013).
31. N. Abdullah, M. A. Rahman, M. H. D. Othman, A. F. Ismail, J. Jaafar and A. A. Aziz, *Ceram. Int.*, **42**, 12312 (2016).
32. C. Zhou, C. Yuan, Y. Zhu, J. Caro and A. Huang, *J. Membr. Sci.*, **494**, 174 (2015).
33. K. Li, Ceramic Membranes for Separation and Reaction, Wiley (2007).
34. F. R. García-García, M. A. Rahman, B. F. K. Kingsbury and K. Li, *Appl. Catal. A Gen.*, **393**, 71 (2011).
35. Q. Wei, F. Zhang, J. Li, B. Li and C. Zhao, *Polym. Chem.*, **1**, 1430 (2010).
36. A. Barras, J. Lyskawa, S. Szunerits, P. Woisel and R. Boukherroub, *Langmuir*, **27**, 12451 (2011).
37. C. V. Mcguire and R. S. Forgan, *Chem. Commun.*, **51**, 5199 (2014).
38. J. Cravillon, R. Nayuk, S. Springer, A. Feldhoff, K. Huber and M. Wiebcke, *Chem. Mater.*, **23**, 2130 (2011).
39. H. Zhang, J. James, M. Zhao, Y. Zhang, B. Zhang and Y. S. Lin, *J. Membr. Sci.*, **532**, 1 (2017).
40. G. T. Gray, J. R. McCutcheon and M. Elimelech, *Desalination*, **197**, 1 (2006).
41. K. M. Gupta, K. Zhang and J. Jiang, *Langmuir*, **31**, 13230 (2015).
42. Z. Hu, Y. Chen and J. Jiang, *J. Chem. Phys.*, **134**, 134705 (2011).
43. D. Fairen-Jimenez, S. A. Moggach, M. T. Wharmby, P. A. Wright, S. Parsons and T. Düren, *J. Am. Chem. Soc.*, **133**, 8900 (2011).